Journal of Alloys and Compounds, 182 (1992) 175–187
JALCOM 135

Lattice parameter of a high purity barium wire extruded in ultrahigh vacuum

Jürgen Evers, Gilbert Oehlinger, Bernd Sendlinger and Armin Weiss
Institut für Anorganische Chemie der Universität München, Meiserstrasse 1, D-8000 München 2 (FRG)

Manfred Schmidt
Rosemount GmbH, Wilhelm-Rohn-Strasse 25, D-6540 Hanau (FRG)

Peter Schramel
Gesellschaft für Strahlen- und Umweltforschung, Ingolstädter Landstrasse 1, D-8042 Neuherberg (FRG)

(Received September 18, 1991)

Abstract

The lattice parameter of high purity barium was determined by the Guinier–Simon technique (Mo Kα_1 radiation; 19 reflections) to 502.8(2) pm at 25 °C. This value is significantly higher than most of the values in the literature.

For the preparation of high purity barium, commercially available metal was distilled in ultrahigh vacuum. The content of metallic impurities was lowered from 99.63 wt.% in the impure metal to 99.99 wt.% in the distilled metal. The major metallic impurity strontium decreased from 3330 to 4 wt.ppm and the major non-metallic impurity hydrogen from 30 to 9 wt.ppm. For X-ray measurements a wire (0.4 mm in diameter and 2 cm long) was extruded at 220 °C in ultrahigh vacuum ($p = 4 \times 10^{-8}$ mbar) and sealed in a silica capillary.

1. Introduction and improved procedure

The lattice parameter of b.c.c. barium shows a considerable scatter from 500.9 to 502.7 pm [1–10]. As a consequence, properties based on the lattice parameter are uncertain: the atomic volume between 62.84×10^6 and 63.52×10^6 pm^3, the metallic radius (coordination number, 8) between 216.9 and 217.7 pm and, finally, the density between 3.590 and 3.629 g cm^{-3}. In most cases, barium of commercial quality was used without further purification at sufficiently inert conditions. The metal was scraped free from oxide in order to obtain a clean sample surface and diffraction experiments were performed with Debye–Scherrer cameras or diffractometers. Since the determination of the lattice parameter by those techniques is precise at least to ±0.2 pm, the scatter for the values in the literature reflects the different purities of the starting samples and their different "histories" of handling during the experiments. The present paper deals with improvements in the

0925-8388/92/$5.00

experimental procedure for determination of the lattice parameter in three steps.

The largest amount of metallic impurities in barium of commercially available quality consists of the alkaline earth (AE) metals. In addition, hydrogen, carbon, nitrogen and oxygen are dissolved in barium. As a first step, ultrahigh vacuum distillation was used as an effective procedure for separation of both metallic and non-metallic impurities [11, 12].

Secondly, ultrahigh-vacuum-distilled barium is highly ductile, thus enabling extrusion of barium wires for diffraction experiments. In an argon glove-box, barium was loaded into an ultrahigh-vacuum-tight wire-extruding apparatus. In order to minimize non-metallic impurities the procedures (wire extrusion and sealing into silica capillaries) were performed under ultrahigh vacuum conditions.

Thirdly, the lattice parameter was determined with high accuracy by the focusing Guinier–Simon technique. Diffraction data were collected on a computer-controlled Guinier diffractometer, which was calibrated against electronic-grade germanium. The exact peak position of each reflection was determined by on-line computer searching of the intensity maximum. The lattice parameter of barium was computed from 19 reflections by a least-squares fit. In addition, the Rietveld method [13] was applied to a second set of diffraction data.

The effect of metallic and non-metallic impurities on the lattice parameter was investigated with different samples: (1) wires of high purity barium sealed in silica capillaries in ultrahigh vacuum; (2) filings of commercially available barium with the usually high amount of metallic and non-metallic impurities, sealed in Lindemann capillaries under argon.

2. Experimental procedure

2.1. Preparation of high purity barium by ultrahigh vacuum distillation and its characterization by inductively coupled plasma emission spectroscopy and vacuum hot extraction

The preparation of high purity barium was carried out in a glove-box in which argon as inert atmosphere is permanently recirculated at a flow rate of 1.7 m^3 h^{-1} by an oil-free compressor. Water and oxygen as residual impurities in argon are removed by flowing the gas through an exterior purification train which contains molecular sieve (Merck 5A) and Oxisorb (silica gel coated with chromium(II)). Removal of the residual impurities hydrogen and nitrogen is performed by flowing the argon through turnings of titanium heated up to 900 °C. Furthermore, by an additional compressor the argon is bubbled through an absorption vessel filled with 300 ml of liquid Na–K alloy. The purity of the argon is controlled by maintaining a lighted electrical lamp with a 2 mm large hole in its bulb. At best conditions the lamp lasts for 4 weeks. Further details of the inert atmosphere system have been given elsewhere [11].

The all-metal ultrahigh vacuum pumping system consists of a large mercury diffusion pump (pumping speed, 170 l s^{-1}; ISO63 flange) and a small pump (pumping speed, 10 l s^{-1}). The small diffusion pump gives a "fore" vacuum of 10^{-7} mbar to the large pump. Cooling is performed by a thermoelectric cooled baffle and two liquid-nitrogen traps (all with ISO63 flanges). After baking to 300 °C the all-metal sealed ultrahigh vacuum system gives a vacuum of the order of 10^{-10} mbar.

The barium was distilled in a double-walled water-cooled silica–Pyrex tube fitted via a CF63 flange to a gate valve. The molybdenum distillation system was heated inductively by high frequency currents of 1 MHz. At its bottom the distillation temperature was 870 °C and at its top 800 °C. Here the high purity metal condensed. The distillation of 100 g of barium took 24 h. Typical vacuum conditions were of the order of 10^{-6}–10^{-7} mbar during distillation and of the order of 10^{-8} mbar in the cold condition. After distillation the silica–Pyrex tube with the high purity metal was locked into the glove-box. Further details of the distillation procedure have been given elsewhere [11].

Trace-analytical characterization for metallic impurities was performed with inductively coupled plasma emission spectroscopy (Instruments S.A., type JY38 with a 1.5 kW high frequency generator at 27 MHz). The apparatus was calibrated chemically by subsequent dilution of Merck Titrisol solutions. Details of the trace-analytical technique have been published elsewhere [14].

By vacuum hot extraction, hydrogen impurities were analysed in a Leybold Evolograph VH9, but unfortunately it is not possible to determine oxygen impurities also by the same procedure. The samples (spheres of 5 mm diameter with about 150 mg mass) of ultrahigh-vacuum-distilled and of Ventron barium were wrapped in platinum foil in the glove-box and then extracted at 850 °C in the Evolograph. Calibration of the gas chromatograph was performed with a test gas of known composition [11].

2.2. *Extruding a wire of high purity barium in ultrahigh vacuum*

Extruding sodium wires under the protective atmosphere of nitrogen is a well-established laboratory technique to dry non-halogenated solvents, *e.g.* ether [15]. The question arose whether the ductility of barium is sufficient to extrude wires in ultrahigh vacuum. Such wires should have a clean surface. Then surface-sensitive X-ray measurements can be applied in order to determine precisely the lattice parameter of barium.

In analogy to the Mohs hardness scale for minerals, Newnham [16] has proposed a hardness scale for metals which ranges from less than 1 to 7. The alkali metals are extremely soft. In this scale they have a hardness less than unity. Because hardness increases with the number of valence electrons the AE metals will have a hardness of 2, and the transition metals a hardness between 4 and 7.

For the extrusion of high purity barium wires a nozzle with a hole of 0.4 mm was used. By applying a load of 2 t, a commercially available sodium extruding apparatus (Tom-Press NPL18, supplied by Fritz Genser, Scientific Instruments, D-8803 Rothenburg o.T., FRG) was successfully tested with lead. Both metals could be cut easily with a pair of pincers in the glovebox.

Figure 1 shows the ultrahigh-vacuum-tight apparatus for wire extrusion. The piston–cylinder apparatus is machined from stainless steel (piston (1) length, 15 mm; cylinder (2) length, 14 cm; inner diameter, 16 mm). With a nut (3) (thread, 22 mm) the nozzle (4) is fixed to the piston–cylinder apparatus. The piston, the inner surface of the cylinder and the nozzle are

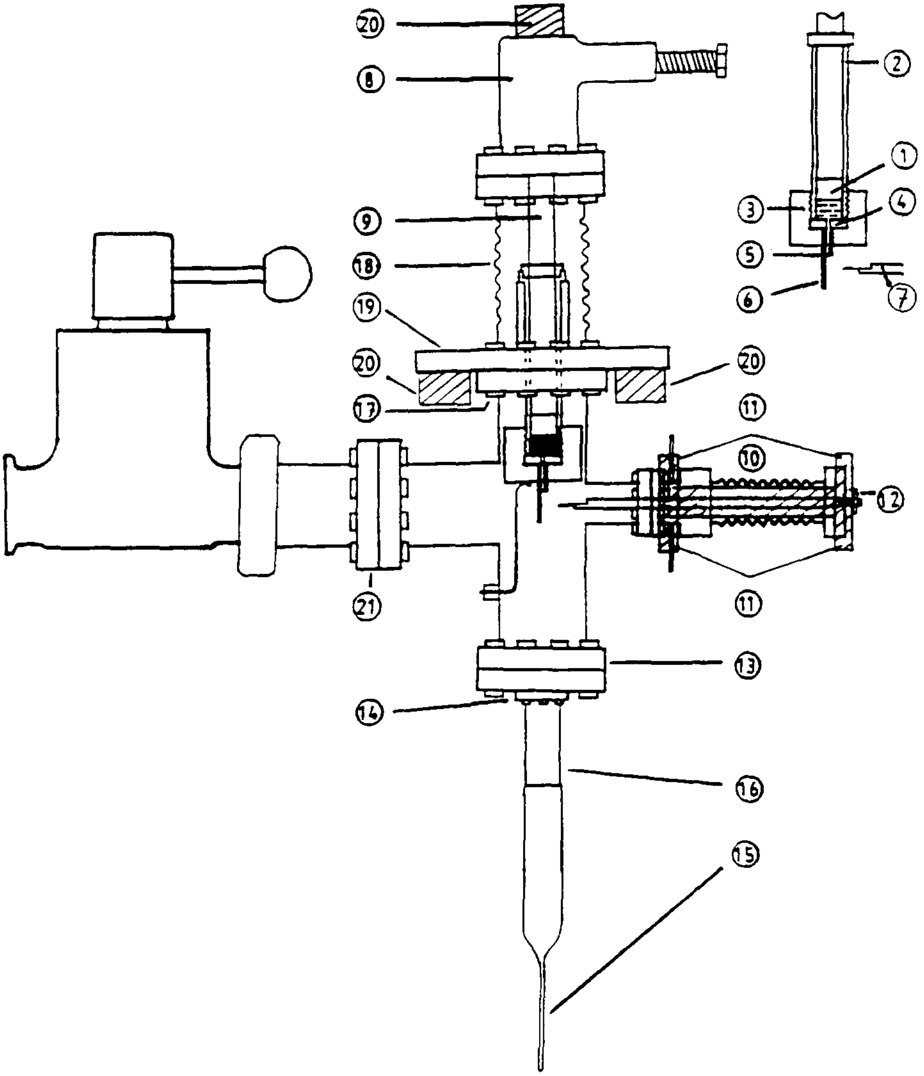

Fig. 1. Schematic drawing of the ultrahigh-vacuum wire-extrusion apparatus. (For reasons of clarity the CF16 viewport is omitted.)

precisely honed. At the lower part of the nut which fixes the nozzle to the cylinder there is a thread rod (5) drilled with a hole of 1 mm. This hole leads the extruded wire to a plate (5 mm × 12 mm) (6) on which it can be cut off by a movable blade (7). The load from a hydraulic press (8) is transmitted by a rod (9) of stainless steel (15 mm diameter; 14 cm length) which fits into the piston (1).

The piston–cylinder apparatus is installed into a stainless steel tee piece with three CF35 flanges. Additionally, the tee piece contains two CF16 flanges: one for a viewport, and the other for the movable blade (7) inside a flexible coupling (10) for cutting off the wire. Against atmospheric pressure which forces the movable blade into the apparatus, it is tightened by a special clip (11), which is fixed with a nut (12). At the lower CF35 flange (13) there is a CF35/16 reducer (14) to which the silica capillary (15) is fitted via a Kovar flange (16). The temperature is measured with a chromel–alumel thermocouple near the plate where the wire is cut off. The upper CF35 flange (17) is connected with a flexible coupling (18) sealed at one end. During extrusion of a wire, this flexible coupling will be contracted and the load is taken up by a special CF35 flange (19) (100 mm outer diameter). This flange is clamped at its lower side in the support of the press (20). The medium CF35 flange (21) is fixed to a bellow-sealed KF40 straight-through valve (leak rate, 10^{-9} mbar l s^{-1}). All flanges are metal sealed, with the exception of the inner seal of the valve which consists of Viton.

The wire extrusion apparatus was locked into the glove-box and filled with 3.5 g (equal to a barium cylinder of 16 mm diameter and 5 mm height) chips of high purity barium. The movable blade (7) and the cutting plate (6) are adjusted to be 90° with respect to each other. Then the apparatus was connected to the ultrahigh-vacuum-pumping system, the tee piece baked at 300 °C and the straight-through valve at 150 °C. After cooling to room temperature a vacuum of the order of 10^{-9} mbar is routine. By external heating to 220 °C the ductility of the high purity barium increased. During the heating period the vacuum decreased by one order of magnitude. For wire extrusion the load was slowly increased within 5 min to 2 t. The ultrahigh vacuum was 4×10^{-8} mbar. When the extruded wire had a length of approximately 2 cm, it was cut off by opening the nut which fixes the clip of the movable blade against the atmospheric pressure. The wire falls down into a silica capillary (1.0 mm diameter; 0.01 mm thickness of the wall) and was sealed by a gas burner in ultrahigh vacuum.

Even by application of pressures up to 2 t, wires of the commercially available barium could not be extruded. Therefore filings of this brittle material were prepared in the glove box, mixed with electronic-grade germanium and then sealed in a Lindemann capillary (0.4 mm diameter).

2.3. Determination of the lattice parameter of high purity and of commercially available barium by the Guinier–Simon technique

The lattice parameter of various barium samples was determined with a computer-controlled Guinier diffractometer (Huber G644) [17] with molybdenum radiation monochromatized by a bent focusing quartz monochromator (Mo Kα_1; 70.9300(1) pm) [18]. This leads to very sharp reflections of high intensity [19, 20]. In comparison with the Debye–Scherrer technique the resolution is doubled. With the improved technique of Simon [21, 22] air-sensitive barium samples in a sealed silica capillary could be investigated without contamination.

The diffractometer was calibrated with electronic-grade germanium (40 Ω cm specific resistivity; $a=565.791(1)$ pm at 25 °C [23]). In the θ range between 5 and 27°, there are observable 13 reflections with $\Sigma\ h^2+k^2+l^2 \leqslant 51$ for germanium, and 19 reflections up to $\Sigma\ h^2+k^2+l^2 \leqslant 40$ for barium. The peak maximum was searched on line by a parabolic fit through 13 data points with highest intensity and an θ increment of 0.003° for every reflection. In Fig. 2 the calibration curve for the diffractometer is plotted [17]. Figure 3 shows the parabolic fit for the 110 reflection of barium and Table 3 (in Section 3) the peak list for 19 reflections after calibration. The lattice parameter of barium was determined with the program LCLSQ [24] by a least-squares procedure.

In addition, 2200 data points were collected with an increment of 0.01° at a counting time of 60 s per point. In the diffractogram with a very low signal-to-noise relation the background was linearized by subtracting a background file from the original data set. The data were corrected for absorption for cylindrical samples [25] with $\mu r=3.3$ and then normalized to an intensity maximum of 500 counts for the strongest reflection and to 25 counts for a linear background. Finally the corrected Guinier diffractogram was analysed by the Rietveld method for the lattice parameter a, the zero-point Z, the half-width parameters u, v and w, the isotropic Debye–Waller factor B, the asymmetry parameter P and the preferred orientation parameters G_1 and G_2 [13]. The preferred orientation was corrected in the Rietveld program by the equation

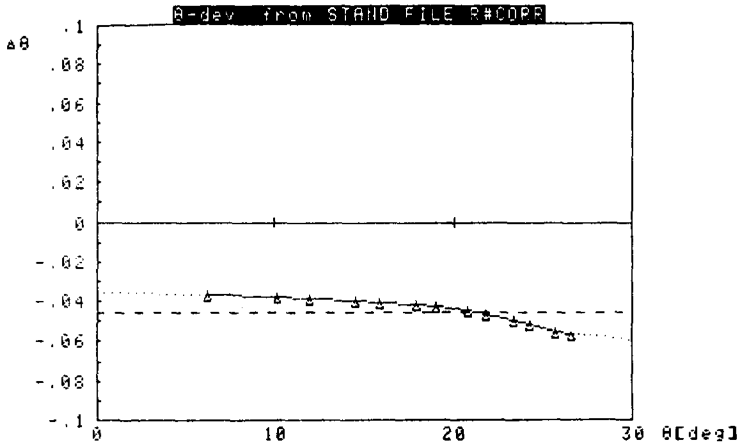

Fig. 2. Calibration curve obtained with electronic grade germanium [23]. On the abscissa the angle θ is shown and on the ordinate the difference from the calculated θ value.

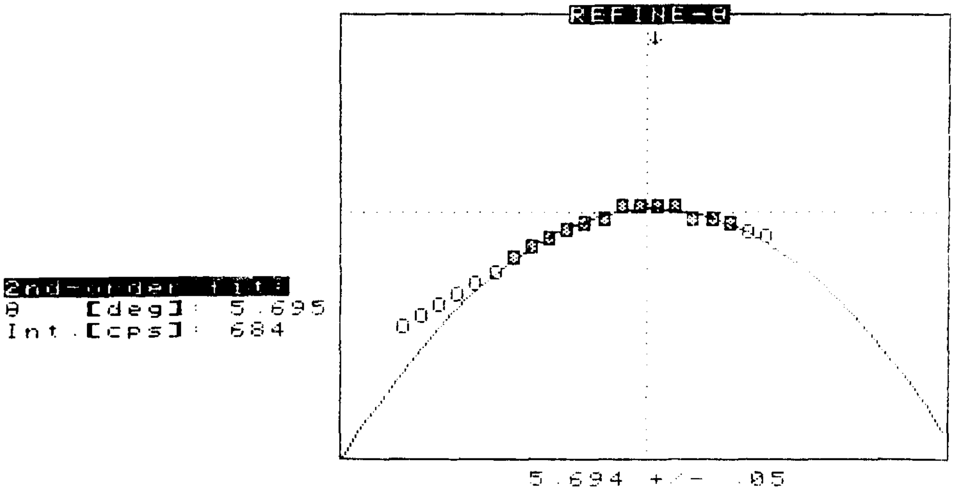

Fig. 3. Parabolic fit from computer searching of the θ position with maximum intensity for the Ba(110) reflection (step scan with an increment of 0.003°).

$$I_{\mathrm{corr}}=I_{\mathrm{obs}}[G_1+(1-G_2)\cdot\exp(-G_1\alpha^2)]$$

where α is the acute angle between the scattering vector and the normal to the crystallites. For calculation of the reflection profiles a modified lorentzian function was used.

The θ positions and the intensity of reflections for additional phases were calculated with the LAZY PULVERIX program [26].

3. Results and discussion

The results of the trace-analytical characterization of the commercially available and of the ultrahigh-vacuum-distilled barium are summarized in Table 1. The large amount of AE metallic impurities in the starting material is a consequence of ionic size and geochemical affinity in the magnesium, calcium, strontium, barium series [11]. Those AE impurities showing the closest resemblance in size to the AE matrix metal are distributed to the greatest. By the purifying process the content of AE impurities was decreased by two orders of magnitude from 3617 to 35 wt.ppm. The highest purification effect was found for strontium impurities by nearly three orders of magnitude: the strontium content was lowered from 3330 to 4 wt.ppm.

The purification effect for hydrogen impurities is much lower than for AE impurities. The hydrogen content of impure barium (with a surface cut free from its white coating in the glove-box) is 30 wt.ppm. The purified metal still contains 9 wt.ppm H (=0.0009 wt.%) which corresponds to 0.062 at.% H (=620 at.ppm). On the assumption that hydrogen is dissolved in barium according to Sievert's law [11, 27]

TABLE 1

Most abundant metallic impurities in commercially available and in ultrahigh-vacuum-distilled barium

Impurity	Content (wt.ppm)	
	Before distillation	After distillation
Mg	17	17
Ca	270	14
Sr	3330	4
Si	4	5
Ti	1	1
Cr	1	1
Mn	29	28
Fe	2	2
Ni	1	1
Cu	12	1
Zn	9	5
Mo	1	1
Sn	15	1
Pb	7	7
Σ	3699	88
Purity (wt.%)	99.63	99.99

The barium sample was supplied by Ventron (catalogue No. 00038; barium rods, 23 mm in diameter).

$$x_H = k_{H,Ba,T} p_{H2}^{1/2}$$

(where x_H is the mole fraction of hydrogen dissolved in barium, $k_{H,Ba,T}$ is the temperature-dependent Sievert's law constant and p_{H2} is the partial pressure of hydrogen during distillation (10^{-7}–10^{-8} mbar)), it becomes evident that p_{H2} has to be lowered by two orders of magnitude to 10^{-9}–10^{-10} mbar in order to decrease x_H by only one order. This partial pressure must be achieved during distillation with the molybdenum distillation column at outgassing conditions between 800 and 870 °C. The pumping speed of the diffusion pump must be increased from 170 l s^{-1} by a factor of 100–17 000 l s^{-1}. Such a large pump requires a flange diameter of 27.5 in (=70 cm), 5 l of pumping fluid and a heating power of 14 kW [28]. Even with modern improved laboratory equipment, it is not easy to lower the hydrogen content in ultrahigh-vacuum-distilled barium by one order of magnitude. In 1971, Rashid and Kayser [9] purified barium by double ultrahigh vacuum distillation. Then they prepared filings under argon, sealed them in a Lindemann capillary and annealed it at 400 K for several days. Nevertheless, they quoted a number of weak small-angle reflections on the Debye–Scherrer photograph and indexed them as BaO and BaH_2 [9]. Also with the improved technique applied in this investigation, traces of BaH_2 were detected in ultrahigh-vacuum-distilled barium (arrow in Fig. 4). The intensity ratio of the strongest barium reflection to these is about 100:1. In Fig. 4 the Rietveld plot [13] of high purity barium is shown.

The lattice parameter a (=502.8(2) pm at 25 °C), the zero-point Z of the diffractometer, the half-width parameters u, v and w, the asymmetry parameter P, the Debye–Waller factor B and the R values are summarized in Table 2. By the Rietveld method the lattice parameter was evaluated for only 18 reflections, because of the remarkable asymmetry of the (110) reflection. In Table 2 the preferred orientation parameters G_1 and G_2 [13] are also presented, since extruding a barium wire at 220 °C leads to partial reorientation of crystallites. This effect was also shown by taking oscillating X-ray diffraction photographs of the wires.

Furthermore, the lattice parameter of high purity barium was computed with the program LCLSQ [24] from 19 on-line refined θ positions. In Table 3 the observed and the calculated 2θ values are shown. Also here the lattice parameter was determined to 502.8(2) pm.

For high purity barium the atomic volume ($63.56(8)\times10^6$ pm^3), the metallic radius for coordination number 8 (217.7(1) pm) and the density (3.588(4) g cm^{-3}) have been computed from the lattice parameter (calculated with an improved value for Avogadro's constant of $6.022\,1363\times10^{23}$ [29] and 137.33 g mol^{-1} [30] for the atomic mass of barium). Only two investigators, both working at the Ames Laboratory of the U.S. Atomic Energy Commission, found lattice parameters near to 502.8(2) pm, determined in this investigation. In 1964, Stevens [7] obtained a=502.6 pm and, in 1971, Rashid and Kayser [9] found a value of a=502.7(2) pm. These three values are significantly higher than most of the data in the literature [1–6]. Therefore it is possible that contamination of barium with special metallic and non-metallic impurities leads to a decrease in the lattice parameter.

In the following the effect of the impurities on the variation in the lattice parameter of barium is discussed.

The metallic radius for coordination number 12 increases in the magnesium, calcium, strontium, barium series (strontium, 215 pm; barium, 224 pm [31]). In 1956, Hirst *et al.* [5] have investigated the Ba–Sr equilibrium system by thermal analysis and by X-ray diffraction [5]. As a result, barium and the smaller AE metal strontium form a continuous series of solid solutions from 0.0 to 69.3 at.% Sr, crystallizing with the b.c.c. structure. Since in this region Vegard's [32] law holds, the lattice parameter of barium decreases with increasing strontium content. Therefore impure barium with 3330 wt.ppm (=0.33 wt.%) Sr must have an apparently lower lattice parameter than that of the high purity metal with only 4 wt.ppm Sr.

The commercially available barium metal is contaminated with two additional phases: BaH_2 and BaO. For this metal a lattice parameter of 501.8(2) pm was derived. Interestingly, this value is very near to those which were derived in earlier experiments for barium samples prepared without further purification and handling under sufficient inert conditions: 500.9–501.5 pm [1–6].

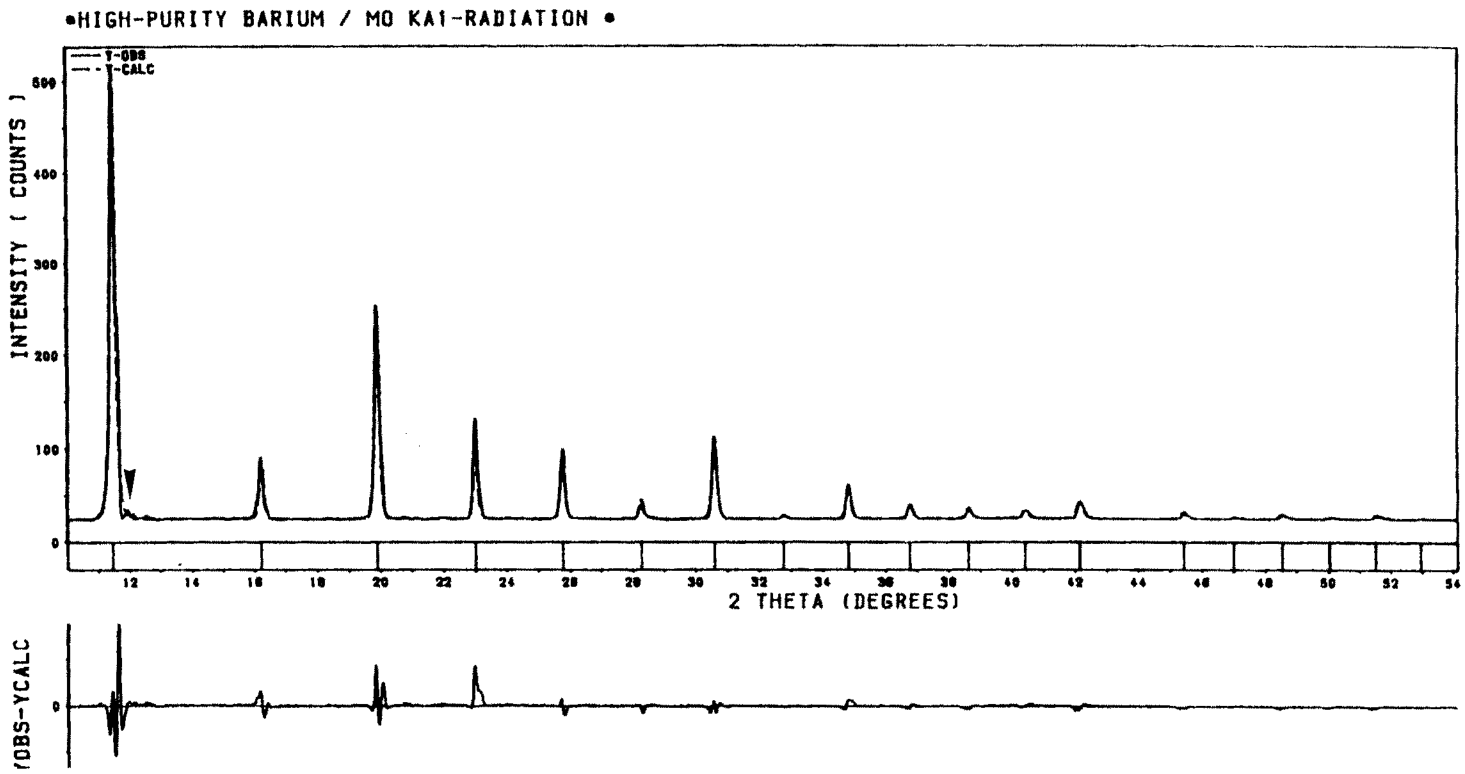

Fig. 4. Observed Guinier diffractogram ($R=6.11\%$) and that calculated by the Rietveld method [13] for high purity barium with Mo $K\alpha_1$ radiation ($2\theta=10$–$54°$; increment, 0.02°; 2200 data points; counting time per point, 60 s). In addition, the position of the reflections and the difference plot between the observed and the calculated diffractograms are shown. The arrow shows the reflections (011) and (102) for BaH_2.

TABLE 2

Data for the Rietveld analysis [13] of the Guinier diffractogram of high purity barium

Lattice parameter a (pm) at 25 °C	502.8(2)
Zero point Z (deg)	0.014(2)
Debye–Waller factor B (Å^2)	1.61(9)
Half-width parameters	
u	1.10(10)
v	−0.46(4)
w	0.071(3)
Asymmetry parameter P	−0.17(4)
Preferred orientation parameters	
G_1	−7.9(16)
G_2	1.7(1)
R values (%)	
R	6.11
R_w	10.69

TABLE 3

Observed and calculated 2θ values, their differences and observed intensities for high purity barium

$h\ k\ l$	$2\theta_{obs}$ (deg)	$2\theta_{calc}$ (deg)	$2\theta_{obs}-2\theta_{calc}$ (deg)	Intensity (observed) (counts)
1 1 0	11.464	11.450	0.014	684
2 0 0	16.202	16.219	−0.017	110
2 1 1	19.894	19.898	−0.004	368
2 2 0	23.016	23.016	0.000	189
3 1 0	25.774	25.776	−0.002	143
2 2 2	28.272	28.285	−0.013	52
3 2 1	30.608	30.605	0.003	201
4 0 0	32.786	32.776	0.010	28
4 1 1	34.836	34.825	0.011	88
4 2 0	36.790	36.775	0.015	49
3 3 2	38.630	38.639	−0.009	38
4 2 2	40.432	40.430	0.002	33
5 1 0	42.152	42.158	−0.006	55
5 2 1	45.450	45.453	−0.003	31
4 4 0	47.036	47.032	0.004	23
5 3 0	48.586	48.571	0.015	28
6 0 0	50.076	50.074	0.002	16
6 1 1	51.524	51.546	−0.022	21
6 2 0	52.988	52.987	0.001	16

The question arose whether the dissolved non-metallic impurities hydrogen and oxygen may affect the cell volume of barium. Unfortunately, sufficient knowledge is still missing about the basic steps in the contamination of bulk barium with such species. Understanding their chemical bonding would then allow their size to be derived. From a comparison of the molar volume of metallic barium with that of its hydride and that of its oxide, one obtains in both cases a volume contraction, but this is true only for total conversion of barium metal into these compounds. As a first rough assumption, it can be imagined that this behaviour holds also for the beginning of compound formation. Thus the lattice parameter of impure barium should then be lower than that for barium which is less contaminated with non-metallic impurities hydrogen and oxygen.

The same effect can be derived from data in the literature [33] for the divalent rare earth (RE) metal europium, remembering that europium and barium show a number of very similar properties (*e.g.* high reactivity against air and moisture, crystal structure and pressure–temperature–phase diagram). In 1956, Barrett [6] determined the lattice parameter for both metals in the same apparatus. For vacuum-distilled europium, a value of $a = 457.7(1)$ pm was derived and, for barium scraped free from oxide, a value of $a = 501$ pm. By an improved experimental procedure [33] at the Ames Laboratory of the U.S. Atomic Energy Commission an a parameter lattice which was nearly 0.6 pm higher ($a = 458.29(4)$ pm) was evaluated for fillings of high purity europium metal. Nevertheless, for barium the difference between the parameter derived for the high purity metal ($a = 502.8(2)$ pm) and that of the less pure metal (501 pm) [6] is tripled to 1.8 pm, simply reflecting the lower purity of the barium sample than the vacuum-distilled europium sample.

For the two other reactive AE metals calcium and strontium, the lattice parameters also show scatter, since earlier investigations were mostly performed on samples which were not purified and handled under sufficient inert conditions. Thus, it is expected that the lattice parameters are higher for purer metals.

Acknowledgments

Financial support by the Fonds der Chemischen Industrie is gratefully acknowledged.

References

1 G. L. Clark, A. J. King and J. F. Hyde, *Proc. Natl. Acad. Sci. U.S.A.*, *14* (1928) 617.
2 A. J. King and G. L. Clark, *J. Am. Chem. Soc.*, *51* (1929) 1709.
3 F. Ebert and H. Hartmann, *Z. Anorg. Allg. Chem.*, *179* (1929) 418.
4 W. Klemm and G. Mika, *Z. Anorg. Allg. Chem.*, *248* (1941) 155.
5 R. G. Hirst, A. J. King and F. A. Kanda, *J. Phys. Chem.*, *60* (1956) 302.
6 C. S. Barrett, *J. Phys. Chem.*, *23* (1956) 1123.
7 R. M. Stevens, *USAEC Rep. TID-20637*, 1964, p. 112 (US Atomic Energy Commission).
8 K.-H. Hellwege and A. M. Hellwege (eds.), Landolt–Börnstein, Neue Serie, Group III, *Kristall- u. Festkörperphysik*, Vol. 6, *Strukturdaten der Elemente und intermetallischen Phasen*, Springer, Berlin, 1971.

9 M. S. Rashid and F. X. Kayser, *J. Less-Common Met.*, *24* (1971) 253.
10 P. Villars and L. D. Calvert, in *Pearson's Handbook of Crystallographic Data for Intermetallic Phases*, American Society for Metals, Metals Park, OH, 1985.
11 J. Evers, G. Oehlinger, A. Weiss, C. Probst, M. Schmidt and P. Schramel, *J. Less-Common Met.*, *81* (1981) 15.
12 J. Evers, A. Weiss, E. Kaldis and J. Muheim, *J. Less-Common Met.*, *30* (1973) 83.
13 D. B. Wiles and R. A. Young, *J. Appl. Crystallogr.*, *14* (1981) 149.
14 P. Schramel, *Spectrochim. Acta, Part B*, *43* (1988) 881.
15 E. Beckmann,. *Chem. Ber.*, *55* (1922) 766.
16 R. E. Newnham, *Structure–Property–Relations*, Springer, Berlin, 1975, p. 199.
17 *Manual for Guinier diffractometer G 644*, Robert Huber, Diffraktionstechnik, Rimsting, 1985.
18 J. A. Bearden, *Rev. Mod. Phys.*, *39* (1967) 78.
19 A. Guinier, *C.R. Acad. Sci.*, *204* (1937) 1115.
20 E.-G. Hofmann and H. Jagodzinski, *Z. Metallkd.*, *46* (1955) 601.
21 A. Simon, *J. Appl. Crystallogr.*, *3* (1970) 11.
22 A. Simon, *J. Appl. Crystallogr.*, *3* (1970) 18.
23 J. F. C. Baker and M. Hart, *Acta Crystallogr.*, *A*, *31* (1975) 364.
24 Ch. W. Burnham, Geophysical Laboratory, Carnegie Institution of Washington, Washington, DC, 1979.
25 K. Sagel, *Tabellen zur Röntgenstrukturanalyse*, Springer, Berlin, 1958.
26 K. Yvon, W. Jeitschko and E. Parthé, *J. Appl. Crystallogr.*, *10* (1977) 73.
27 A. W. Searcy and L. N. Finney, in V. F. Zackay (ed.), *High Strength Materials*, Wiley, New York, 1965, p. 104.
28 *Varian Catalogue*, Varian (Vacuum Division), Palo Alto, CA, Chapters 2 and 6.
29 P. Seyfried, to be published.
30 R. C. Weast (ed.), CRC Handbook of Chemistry and Physics, 69th edn., 1988–1989, CRC Press, Boca Raton, FL, 1988.
31 W. B. Pearson, *The Crystal Chemistry and Physics of Metals and Alloys*, Wiley-Interscience, New York, 1972.
32 L. Vegard, *Z. Phys.*, *5* (1921) 17.
33 B. J. Beaudry and P. E. Palmer, *J. Less-Common Met.*, *34* (1974) 225.